

Structure of the Molybdenum Site of Dimethyl Sulfoxide Reductase

Graham N. George,^{*,†} James Hilton,[‡] Carrie Temple,[‡] Roger C. Prince,[§] and K. V. Rajagopalan[‡]

Contribution from the Stanford Synchrotron Radiation Laboratory, SLAC, Stanford University, P.O. Box 4349, MS 69, Stanford, California 94309, Department of Biochemistry, School of Medicine, Duke University, Durham, North Carolina 27710, and Exxon Research and Engineering Company, Route 22 East, Annandale, New Jersey 08801

Received August 10, 1998

Abstract: Molybdenum K-edge X-ray absorption and Mo(V) electron paramagnetic resonance (EPR) spectroscopies have been used to probe the metal coordination in oxidized and reduced forms of both wild-type and a site-directed mutant of *Rhodobacter sphaeroides* dimethyl sulfoxide (DMSO) reductase. We confirm our earlier findings (George, G. N.; Hilton, J.; Rajagopalan, K. V. *J. Am. Chem. Soc.* 1996, 118, 1113–1117) that the molybdenum site of the oxidized Mo(VI) enzyme possesses one terminal oxygen ligand (Mo=O) at 1.68 Å, four thiolate ligands at 2.44 Å, and one oxygen at 1.92 Å and that the dithionite-reduced Mo(IV) enzyme possesses a desoxo species with three or four Mo–S at 2.33 Å and two different Mo–O ligands at 2.16 and 1.92 Å. Mo(V) EPR indicates the presence of one exchangeable oxygen ligand, most likely an Mo–OH, in the signal-giving species, probably originating from the Mo=O of the oxidized enzyme ($E_{m8.5}(IV/V) = +37$ mV, $E_{m8.5}(V/VI) = +83$ mV). The addition of dimethyl sulfide, in the reverse of the physiological reaction, reduces the enzyme. In this form, the enzyme contains a desoxo active site with four Mo–S at 2.36 Å and two different Mo–O ligands at 1.94 and 2.14 Å. Recombinant wild-type *R. sphaeroides* DMSO reductase expressed in *Escherichia coli* initially has a dioxo structure (two Mo=O at 1.72 Å and four Mo–S at 2.48 Å) but assumes the wild-type Mo(VI) structure after a cycle of reduction and reoxidation. The site-directed Ser147→Cys mutant possesses a monooxo active site in the oxidized state (Mo=O at 1.70 Å) with five sulfur ligands (at 2.40 Å), consistent with cysteine 147 coordination to Mo. The dithionite reduced form of the mutant possesses a desoxo site also with five Mo–S ligands (at 2.37 Å) and one Mo–O at 2.12 Å. The variant has substantially different Mo(V) EPR and electrochemistry ($E_{m8.5}(IV/V) = -43$ mV, $E_{m8.5}(V/VI) = +106$ mV). The active-site structure and catalytic mechanism of DMSO reductase are discussed in the light of these results.

Introduction

The mononuclear molybdenum enzymes all possess one or two molybdopterin dithiolene cofactors¹ coordinated to the metal (Figure 1) yet exhibit remarkably diverse functionalities.² Nevertheless, the majority that have been characterized to date catalyze two-electron redox reactions coupled to the transfer of an oxygen atom to or from water.³ During the catalytic cycle, the molybdenum cycles between Mo(VI) and Mo(IV) oxidation states. For example, dimethyl sulfoxide (DMSO) reductase catalyzes the reduction of dimethyl sulfoxide to dimethyl sulfide:

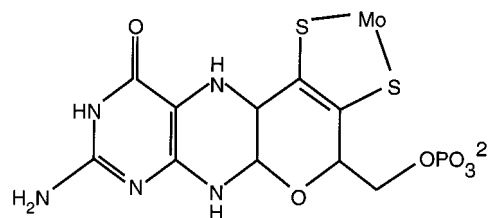
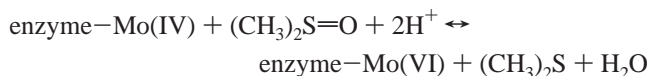


Figure 1. Proposed minimal structure of the molybdenum cofactor. The reversible formation of tricyclic via the formation of a pyran ring through attack of the 3'-OH at C-7 of a dihydropyridine has been proposed. In enzymes from prokaryotic sources, the cofactor can have a dinucleotide moiety (cytosine, adenine, or guanine dinucleotides are known) attached via the pyrophosphate linkage.

Until recently,^{8–12} structural information on molybdenum enzymes was derived almost entirely from spectroscopic studies of the enzymes and of model compound systems.² Two

(3) Molybdenum enzymes have previously been described as all involving two-electron redox chemistry at molybdenum, coupled with the transfer of an oxygen atom. While this rule still appears to hold for most molybdenum enzymes and for their close relatives the tungsten enzymes, it now seems that there are exceptions. The recently discovered tungsten enzyme acetylene hydratase⁴ catalyzes a net hydration reaction rather than a redox one, and formate oxidation to CO₂ by *Escherichia coli* formate dehydrogenase H does not involve oxygen atom transfer.⁵ Furthermore, the presence of the potentially redox-active selenosulfide at the active site⁶ suggests that the molybdenum in formate dehydrogenases might not be redox active during the catalysis.⁷

[†] Stanford Synchrotron Radiation Laboratory.

[‡] Duke University.

[§] Exxon Research and Engineering Company.

(1) (a) Rajagopalan, K. V. *Adv. Enzymol. Relat. Areas Mol. Biol.* 1991, 64, 215–290. (b) Rajagopalan, K. V.; Johnson, J. L. *J. Biol. Chem.* 1992, 267, 10199–10202.

(2) (a) Kisker, C.; Shindelin, H.; Rees, D. C. *Annu. Rev. Biochem.* 1997, 66, 233–267. (b) Hille, R. *Chem. Rev.* 1996, 96, 6, 2757–2816. (c) Johnson, M. K.; Rees, D. C.; Adams, M. W. W. *Chem. Rev.* 1996, 96, 6, 2817–2859. (d) Hille, R. *Biochim. Biophys. Acta* 1994, 1184, 143–169. (e) Enemark, J. H.; Young, C. G. *Adv. Inorg. Chem.*, 1993, 40, 1–88. (f) Wootton, J. C.; Nicolson, R. E.; Cock, M. J.; Walters, D. E.; Burke, J. F.; Doyle, W. A.; Bray, R. C. *Biochim. Biophys. Acta* 1993, 1057, 157–185. (g) Enemark, J. H.; Young, C. G. *Adv. Inorg. Chem.* 1993, 40, 1–88.

spectroscopic methods have proved particularly valuable: Mo(V) electron paramagnetic resonance (EPR) spectroscopy and Mo K-edge X-ray absorption spectroscopy (XAS). There are now three independent reports of crystal structures of DMSO reductase from two closely related prokaryotes: *Rhodobacter sphaeroides* and *Rhodobacter capsulatus*.^{9–12} All three structures confirm that the enzyme contains two pterin dithiolene cofactors and show nearly identical folds for the polypeptide chains^{9–12} with a protein serine ligand (Ser147) on molybdenum. Despite these similarities, the three crystal structures show strikingly different molybdenum ligations including disparities in the number of Mo=O groups and the nature of the dithiolene coordination. In addition to the crystallographic studies, both the *R. sphaeroides* and *R. capsulatus* enzymes have been the objects of previous studies by XAS,^{13,14} resonance Raman,^{15,16} magnetic circular dichroism,^{17,18} UV-visible,^{15–19} and EPR^{19,20} spectroscopies. In contrast to what might be expected from the crystal structures, many of the reported spectroscopic properties of the *R. sphaeroides* and *R. capsulatus* DMSO reductases are very similar.

As recently discussed by Rees and co-workers,²¹ there are problems with discerning the details of metalloprotein active sites by X-ray crystallography, especially when the metal is a large one such as molybdenum. X-ray absorption spectroscopy provides a complementary tool that can accurately measure metal–ligand bond lengths, which are difficult to determine exactly by crystallography.²¹

Our previous X-ray absorption spectroscopy of *R. sphaeroides* DMSO reductase,¹³ indicated a monooxo Mo(VI) site with about

four Mo–S ligands and a desoxo Mo(IV) site with three or four Mo–S ligands. The crystal structure subsequently reported by Schindelin et al.⁹ is in qualitative (but not quantitative) agreement with this, as is a recent resonance Raman spectroscopic study.¹⁶ In contrast, Garner and co-workers have reported an X-ray absorption spectroscopic study of *R. capsulatus* DMSO reductase consistent with the crystallographic work of McAlpine et al.¹⁴ A third structure with only one of the two pterin dithiolenes coordinated to molybdenum had previously been reported for *R. capsulatus* DMSO reductase by Schneider et al.¹⁰ In an attempt to resolve the controversy concerning the structure of the active site, we present a detailed study of the molybdenum site of recombinant wild-type and native wild-type *R. sphaeroides* DMSO reductase and of a Ser147→Cys variant, using both Mo K-edge and sulfur K-edge XAS and Mo(V) EPR spectroscopy.

Materials and Methods

Samples. The brown *R. sphaeroides* DMSO reductase was purified as previously described.²² The previously cloned *R. sphaeroides* DMSO reductase gene²³ was used for obtaining the recombinant enzyme. Details of the heterologous expression of the enzyme and its S147C mutant in *Escherichia coli* and characterization of the purified proteins will be described elsewhere (Hilton, J.; Temple, C.; Rajagopalan, K. V. *J. Biol. Chem.* In press). Briefly, upon purification from the *E. coli* cells, the recombinant wild-type (WT) enzyme is green and displays an absorption spectrum different from that of the protein purified from *R. sphaeroides* cells. However, after a reduction and reoxidation cycle, the enzyme is indistinguishable from the native protein either in color or in its absorption spectrum. Replacement of serine 147, a ligand of the Mo, with cysteine by site-directed mutagenesis followed by expression in *E. coli* produces a viable, salmon-colored protein containing the bis(MGD)Mo cofactor. Analysis of the activity of the S147C variant using several substrates (Hilton, J., Temple, C. and Rajagopalan, K. V., *J. Biol. Chem.* In press) has shown that although this substitution leads to losses of 61–99% of activity toward five substrates, the adenine *N*-oxide reductase activity increases by a factor of 5.

EPR Spectroscopy. Electron paramagnetic resonance (EPR) spectroscopy and data reduction were performed as described by George et al.²⁴ Redox titrations followed the method of Dutton²⁵ using 40 μ M *N*-methylphenazonium methosulfate, *N*-ethylphenazonium ethiosulfate, 2-hydroxy-1,4-naphthoquinone, 2-hydroxy-1,4-anthraquinone, indigo disulfonate, indigo trisulfonate, and benzyl viologen as redox mediators between the protein and the platinum measuring electrode. Potentials were measured with respect to a saturated calomel electrode but are reported with respect to the hydrogen electrode by assuming that the calomel electrode has a potential of +247 mV.²⁶

XAS Data Collection. XAS measurements were carried out at the Stanford Synchrotron Radiation Laboratory with the SPEAR storage ring containing 55–100 mA at 3.0 GeV. Molybdenum K-edge data were collected on beamline 7-3 using a Si(220) double-crystal monochromator, with an upstream vertical aperture of 1 mm, and a wiggler field of 1.8 T. Harmonic rejection was accomplished by detuning one monochromator crystal to approximately 50% off peak, and no specular optics were present in the beamline. The incident X-ray intensity was monitored using an argon-filled ionization chamber, and X-ray absorption was measured as the X-ray Mo K α fluorescence excitation spectrum using an array of 13 germanium intrinsic detectors.²⁷ During data collection, samples were maintained at a temperature of ap-

- (4) Rosner, B. M.; Schink, B. J. *Bacteriol.* **1995**, *177*, 5767–5772.
 (5) Khangulov, S. V.; Gladyshev, V. N.; Dismukes, G. C.; Stadtman, T. C. *Biochemistry* **1998**, *37*, 3518–3528.
 (6) George, G. N.; Colangelo, C. M.; Dong, J.; Scott, R. A.; Khangulov, S. V.; Gladyshev, V. N.; Stadtman, T. C. *J. Am. Chem. Soc.* **1998**, *120*, 1267–1273.
 (7) George, G. N.; Moura, I.; Moura, J. J., Unpublished observations.
 (8) (a) Romão, M. J.; Archer, M.; Moura, I.; Moura, J. J. G.; LeGall, J.; Engh, R.; Schneider, M.; Hof, P.; Huber, R. *Science* **1995**, *270*, 1170–1176. (b) Huber, R.; Hof, P.; Duarte, R. O.; Moura, J. J. G.; Moura, I.; Liu, M.-H.; LeGall, J.; Hille, R.; Archer, M.; Romão, M. J. *Proc. Natl. Acad. Sci. U.S.A.* **1996**, *93*, 8846–8851. (c) Boyington, J. C.; Gladyshev, V. N.; Khangulov, S. V.; Stadtman, T. C.; Sun, P. D. *Science* **1997**, *275*, 1305–1308. (d) Kisker, C.; Schindelin, H.; Pacheco, A.; Wehbi, W. A.; Garrett, R. M.; Rajagopalan, K. V.; Enemark, J. E.; Rees, D. C. *Cell* **1997**, *91*, 1–20.
 (9) Schindelin, H.; Kisker, C.; Hilton, J.; Rajagopalan, K. V.; Rees, D. C. *Science* **1996**, *272*, 1615–1621.
 (10) Schneider, F.; Löwe, J.; Huber, R.; Schindelin, H.; Kisker, C.; Knäblein, J. *J. Mol. Biol.* **1996**, *263*, 53–69.
 (11) McAlpine, A. S.; McEwan, A. G.; Shaw, A. L.; Bailey, S. *J. Biol. Inorg. Chem.* **1997**, *2*, EXAFS 690–701.
 (12) McAlpine, A. S.; McEwan, A. G.; Bailey, S. *J. Mol. Biol.* **1998**, *275*, 613–623.
 (13) George, G. N.; Hilton, J.; Rajagopalan, K. V. *J. Am. Chem. Soc.* **1996**, *118*, 1113–1117.
 (14) Baugh, P. E.; Garner, C. D.; Charnock, J. M.; Collison, D.; Davies, E. S.; McAlpine, A. S.; Bailey, S.; Lane, I.; Hanson, G. R.; McEwan, A. G. *J. Biol. Inorg. Chem.* **1997**, *2*, 634–643.
 (15) (a) Gruber, S.; Kilpatrick, L.; Bastian, N. R.; Rajagopalan, K. V.; Spiro, T. G. *J. Am. Chem. Soc.* **1990**, *112*, 8179–8180. (b) Kilpatrick, L.; Rajagopalan, K. V.; Hilton, J.; Bastian, N. R.; Steifel, E. I.; Pilato, R. S.; Spiro, T. G. *Biochemistry* **1995**, *34*, 3032–3039.
 (16) Garton, S. D.; Hilton, J.; Hiroyuki, O.; Crouse, B. R.; Rajagopalan, K. V.; Johnson, M. K. *J. Am. Chem. Soc.* **1997**, *119*, 12906–12916.
 (17) Benson, N.; Farrar, J. A.; McEwan, A. G.; Thomson, A. J. *FEBS Lett.* **1992**, *307*, 169–172.
 (18) Finnegan, M. G.; Hilton, J.; Rajagopalan, K. V.; Johnson, M. K. *Inorg. Chem.* **1993**, *32*, 2616–2617.
 (19) Bastian, N. R.; Kay, C. J.; Barber, M. J.; Rajagopalan, K. V. *J. Biol. Chem.* **1991**, *266*, 45–51.
 (20) Bennet, B.; Benson, N.; McEwan, A. G.; Bray, R. C. *Eur. J. Biochem.* **1994**, *255*, 321–331.
 (21) Schindelin, H.; Kisker, C.; Rees, D. C. *J. Biol. Inorg. Chem.* **1997**, *2*, 773–781.

- (22) Hilton, J.; Rajagopalan, K. V. *Arch. Biochem. Biophys.* **1996**, *325*, 139–143.
 (23) Hilton, J. C.; Rajagopalan, K. V. *Biochim. Biophys. Acta, Gene Struct. Expr.* **1996**, *1294*, 111–114.
 (24) George, G. N.; Prince, R. C.; Kipke, C. A.; Sunde, R. A.; Enemark, J. E. *Biochem. J.* **1988**, *256*, 307–309.
 (25) Dutton, P. L. *Methods Enzymol.* **1978**, *24*, 431–446
 (26) Clark, W. M. *Oxidation-Reduction Potentials of Organic Systems*; Williams and Wilkins: Baltimore, MD, 1960.
 (27) Cramer, S. P.; Tench, O.; Yocum, M.; George, G. N. *Nucl. Instrum. Methods Phys. Res.* **1988**, *A266*, 586–591.

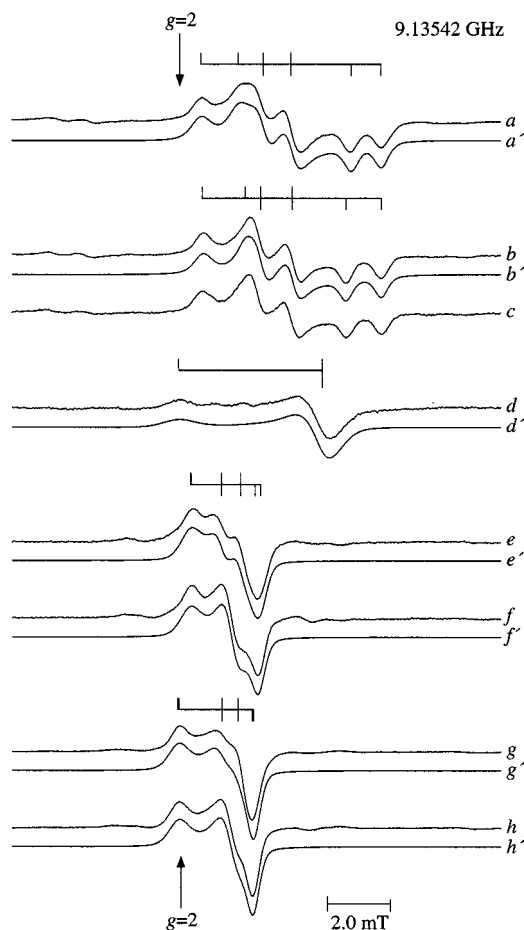


Figure 2. DMSO reductase Mo(V) EPR spectra. Traces a–h are experimental spectra while traces a'–h' are computer simulations (see Table 1 for parameters). Trace a shows the EPR spectrum obtained from reductive titrations of native wild-type (WT) DMSO reductase, and traces b and c show the EPR spectra obtained from oxidative titrations of native WT (b) or recombinant WT enzyme (c). Traces d–h show the Mo(V) EPR spectra from the DMSO reductase Ser147→Cys (S147C) variant in H₂O (d, e, g) and in ²H₂O (f, h). Trace d shows the minor S147C EPR signal, while traces e–h show the major S147C EPR signal at pH 8.5 (e, f) and at pH 6.5 (g, h).

proximately 10 K, using an Oxford Instruments liquid helium flow cryostat. For each sample, eight to ten 35 min scans were accumulated, and the absorption of a molybdenum metal foil was measured simultaneously by transmittance. The energy was calibrated with reference to the lowest energy inflection point of the molybdenum foil, which was assumed to be 20003.9 eV.

XAS Data Analysis. The extended X-ray absorption fine structure (EXAFS) oscillations $\chi(k)$ were quantitatively analyzed by curve-fitting the weighted k -space data using the EXAFSPAK suite of computer programs^{28,29} employing ab initio theoretical phase and amplitude functions generated with the program FEFF version 7.02.³⁰ No smoothing, Fourier filtering, or related manipulations were performed upon the data.

Results

Mo(V) EPR Spectra. Figure 2 shows the Mo(V) EPR spectra of native WT, recombinant WT, and S147C variant DMSO

reductases together with computer simulations. The spin Hamiltonian parameters extracted by simulation are summarized in Table 1. Figure 2a shows the Mo(V) EPR spectrum of native WT enzyme during reductive redox titrations of oxidized, as isolated, enzyme. Identical line shapes were obtained by addition of 1 mM (final) dithionite and freezing the sample prior to full equilibration (i.e., within ~10 s) as previously described by Bennet et al.²⁰ Subtly different spectra (Figure 2b) were observed upon oxidative titration of reduced enzyme and upon subsequent reductive titrations. This suggests that reduction and reoxidation in the absence of substrate cause slight changes in the molybdenum coordination environment, most likely a subtle conformational change. Redox titration of the native WT enzyme (Figure 3A) indicated midpoint potentials at pH 8.5 of +37 and +87 mV for the Mo(IV/V) and Mo(V/VI) couples, respectively. These are in excellent agreement with the values determined by Bastian et al.,¹⁹ allowing for the expected change in midpoint potential of –59 mV per pH unit. We did not observe the pH-dependent degradation and broadening of the Mo(V) EPR signals reported by Bastian et al.¹⁹ No Mo(V) EPR signals were observed when the enzyme was reduced with dimethylsulfide (DMS), either at stoichiometric or at substoichiometric concentrations. Mo(V) EPR signals identical in form to the spectrum of Figure 2a were observed when DMS-reduced enzyme was allowed to partially reoxidize in air at room temperature for approximately 20 min.

Recombinant WT *R. sphaeroides* DMSO reductase as isolated from *E. coli* clearly differs from enzyme isolated from *R. sphaeroides* in being a distinctive green instead of the characteristic brown of the native WT enzyme. The recombinant protein gave no Mo(V) EPR spectra with reductive redox titrations (starting from the green, as isolated, enzyme) or by timed additions of dithionite.²⁰ However, after reduction of the sample to –150 mV, subsequent reoxidation gave Mo(V) EPR signals that were indistinguishable from those of the native WT enzyme isolated from *R. sphaeroides* (Figure 2c) with essentially identical midpoint potentials (not illustrated). This reductively conditioned recombinant WT enzyme now had the characteristic brown color of the native WT enzyme, and the optical spectra were indistinguishable.

The Mo(V) EPR spectra of the native WT enzyme are similar to those reported previously for this enzyme by Bastian et al.¹⁹ and the high- g split species observed with *R. capsulatus* DMSO reductase by Bray and co-workers.²⁰ In agreement with both these studies, preparation of the sample in ²H₂O caused loss of the resolved proton hyperfine structure (not illustrated). In addition to the high- g split signals, Bray and co-workers observed some quite different Mo(V) EPR signals which they called low- g types 1 and 2. The low- g type 1 is of particular interest in that it resembled the slow signal of desulfo xanthine oxidase. Despite extensive efforts, we were unable to produce these signals in our preparations of *R. sphaeroides* DMSO reductase, although small quantities (~5%) of a new Mo(V) EPR signal were obtained when samples were left overnight at room temperature. This new signal (not illustrated), which is presumed to originate from degraded enzyme, had $g_{xyz} = 1.9520, 1.9806, 1.9922$ and no resolved proton hyperfine structure.

As discussed previously,^{13,19,20} the exchangeable coupled proton of the native WT DMSO reductase high- g split Mo(V) EPR signal (Figure 2a,b) is likely due to Mo–O–H ligation. Mo(V) spin Hamiltonian parameters are very sensitive to structure,^{31,32} and thus the similarity in EPR parameters indicates

(28) The EXAFSPAK program suite was developed by G.N.G. and is available from <http://ssrl.slac.stanford.edu/exafspak.html>.

(29) George, G. N.; Kipke, C. A.; Prince, R. C.; Sunde, R. A.; Enemark, J. H.; Cramer, S. P. *Biochemistry* **1989**, *28*, 5075–5080.

(30) (a) Rehr, J. J.; Mustre de Leon, J.; Zabinsky, S. I.; Albers, R. C. *J. Am. Chem. Soc.* **1991**, *113*, 5135–5140. (b) Mustre de Leon, J.; Rehr, J. J.; Zabinsky, S. I.; Albers, R. C. *Phys. Rev.* **1991**, *B44*, 4146–4156.

(31) E.g., see: George, G. N.; Bray, R. C. *Biochemistry* **1988**, *27*, 3603–3609.

Table 1. Mo(V) EPR Spin-Hamiltonian Parameters^a

	$g_{x,y,z} (\Delta^b)$			g_{av}	$A_{x,y,z}^c$		
	x	y	z		x	y	z
wild-type 1	1.9645 (0.28)	1.9813 (0.30)	1.9924 (0.38)	1.9793	¹ H 26.1 ¹⁷ O 4.1 (44°)	24.5 28.0 (0°)	33.3 5.0 (25°)
wild-type 2	1.9650 (0.25)	1.9815 (0.27)	1.9916 (0.34)	1.9794	¹ H 30.7	27.8	38.0
S147C pH8.5 (minor)		1.9729 (0.58)	2.0004 (0.60)	1.9821			
S147C pH8.5 (major)	1.9851 (0.25)	1.9903 (0.27)	1.9981 (0.38)	1.9912	¹ H 4.9	16.8	~0.7
S147C pH6.5 (major)	1.9861 (0.24)	1.9905 (0.32)	2.0005 (0.38)	1.9924	¹ H ~1.5	14.0	~0.9

^a Spin-Hamiltonian parameters were refined by least-squares fitting to the experimental spectra. ^b Values for half line widths in mT are given in parentheses. ^c Values for hyperfine couplings are in MHz, and the values in parentheses are the angles of noncollinearity, α , β , and γ .

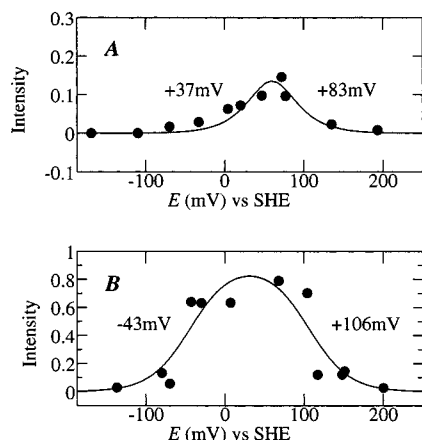


Figure 3. Potentiometric titrations of (A) native WT and (B) S147C DMSO reductases at pH 8.5. In both cases, the ordinate is the integrated intensity of the Mo(V) EPR signal and corresponds to the (approximate) fraction of total Mo present as Mo(V).

that the structural differences among all the different *R. sphaeroides* and *R. capsulatus* DMSO reductase high- g split signal-giving species are very small.

Three different Mo(V) EPR signals were observed with S147C DMSO reductase. Brief exposure to excess dithionite at pH 8.5 produced the low-intensity (approximately 5% Mo(V)) axial signal shown in Figure 2d. Small contributions from this signal were also observed in redox titrations, and these diminished after the sample had been poised at low potential. The major signal observed in redox titrations is shown in Figure 2e–g. This signal is unique among DMSO reductase Mo(V) EPR spectra in showing sensitivity to pH. Redox titration (Figure 3) indicated midpoint potentials at pH 8.5 of -43 and $+106$ mV for the Mo(IV/V) and Mo(V/VI) couples, respectively. Limited redox potentiometric measurements at pH 6.5 suggested that the midpoint potentials at least approximately followed the expected pH dependency. Preparation of the sample in ²H₂O caused loss of the proton hyperfine structure (Figure 2f,h), and computer simulations indicate a rather lower g anisotropy than observed with other DMSO reductase Mo(V) EPR signals^{19,20} (Table 1), with a more anisotropic hyperfine coupling to a single exchangeable proton (Table 1).

A similar substitution of cysteine for the Mo-coordinated serine in *E. coli* DMSO reductase also causes significant changes in the Mo(V) EPR.³³ Several new Mo(V) species with high g values were observed, together with a shift of approximately $+100$ mV for both Mo(IV)/Mo(V) and Mo(V)/Mo(VI) midpoint potentials.³³ This contrasts somewhat with our midpoint potential shifts of -80 mV and $+23$ mV for the Mo(IV)/Mo(V) and Mo-

(V)/Mo(VI) midpoint potentials, respectively, but the structural nature of the *E. coli* DMSO reductase molybdenum site is currently uncertain, and the Mo(V) EPR is quite distinct from that of the *R. capsulatus* and *R. sphaeroides* enzymes, so the *E. coli* and *Rhodobacter* enzymes may have somewhat different active sites.

The EXAFS data, discussed below, indicate that redox-conditioning of the active site also occurs for the S147C variant, and it is possible that the low-intensity S147C Mo(V) EPR (Figure 2d) may be associated with pre-redox-conditioned enzyme. While the exact origin of this signal is uncertain, the g value trends of the major S147C signal (Figure 2e,f) seem to indicate increased Mo–S ligation in the signal-giving species. Increased g values are expected with increased sulfur coordination due to spin–orbit coupling with filled sulfur orbitals. Cleland et al.³⁴ reported Mo(V) EPR spectra from a range of Mo(V) complexes with systematic variation of molybdenum ligation and found an increase in g_{av} of approximately $+0.015$ for one O \rightarrow S substitution. This is in accord with the difference between the native WT and S147C Mo(V) g_{av} of $+0.013$ (signal 2, $+0.0128$ at pH 8.5, $+0.0131$ at pH 6.5). Thus, the higher g values of the S147C mutant suggest that C147 is indeed a ligand of Mo in the signal-giving species. The more prominent signal (Figure 2e,f) is, however, rather unusual in possessing a very low g anisotropy ($g_x - g_z = 0.0130$ at pH 8.5 and 0.0144 at pH 6.5), in fact lower than any other reported molybdenum enzyme Mo(V) EPR signal aside from the desulfo inhibited xanthine oxidase Mo(V) EPR signal.²

Anisotropy in g has its origins in the spin–orbit coupling of the ground-state molecular orbital to the other vacant metal 4d levels and to ligand-based filled orbitals. This can be described by eq 1, where g_e is the free-electron g value (2.002 32), ξ_{Mo} is

$$g_i = g_e - \frac{\xi_{Mo} F}{\Delta E_m} + \frac{\xi_{Mo} G}{\Delta E_l} \quad (1)$$

the one-electron spin–orbit coupling constant for an electron in a molybdenum 4d orbital, ΔE_m is the energy associated with a d–d transition, and ΔE_l is that associated with a one-electron excitation from a filled ligand orbital to metal 4d orbital. The forms of the constants F and G are discussed elsewhere.³² The second term in eq 1 gives rise to the positive contribution to g observed with sulfur ligation, discussed above. In the case of molybdenyl $[Mo=O]^{3+}$ complexes, which comprise the bulk of the model compound literature, the Mo=O bond causes large ligand field splittings with the half-occupied ground state oriented such that Mo=O is oriented along its double node. If the metal contribution in eq 1 dominates, we expect $g_z < g_x, g_y$, but for thiolate-rich $[Mo=O]^{3+}$ complexes, the ligand terms reverse this, causing $g_z > g_x, g_y$. In the case of a desoxo Mo-

(32) E.g., see: Balagopalkrishna, C.; Kimbrough, J. T.; Westmoreland, D. T. *Inorg. Chem.* **1996**, *35*, 7758–7768.

(33) Trieber, C. A.; Rothery, R. A.; Weiner, J. H. *J. Biol. Chem.* **1996**, *271*, 27339–27345.

(34) Cleland, W. E.; Barnhardt, I. T. M.; Yamanouchi, K.; Collison, D.; Mabbs, F. E.; Ortega, R.; Enemark, J. H. *Inorg. Chem.* **1987**, *26*, 1017–1025.

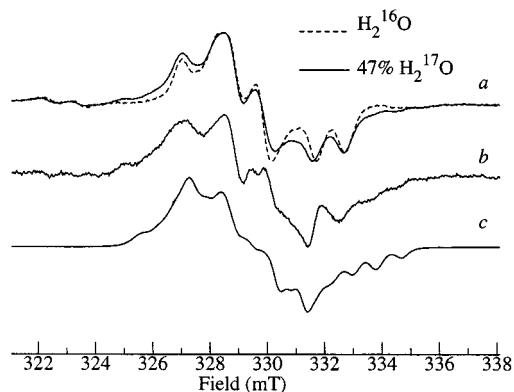


Figure 4. Effects of enrichment in H_2^{17}O upon the native WT DMSO reductase type 1 Mo(V) EPR spectrum. Traces a show the control in H_2^{16}O (natural abundance) water (broken line) and the spectrum of DMSO reductase in 47% enriched H_2^{17}O . Trace b shows a difference spectrum generated from the traces shown in (a), corresponding to one coupled exchangeable oxygen, and trace c shows a computer simulation of (b) using the parameters given in Table 1.

(V) species, ΔE_m will be smaller than with molybdenyl complexes (especially with a coordination environment dominated by thiolate ligands), and the effects of the first term in eq 1 will therefore be more significant than with molybdenyl complexes. Thus, it is possible that, for S147C DMSO reductase, the opposing ligand and metal contributions in eq 1 partially cancel each other and conspire to cause an effectively smaller than normal g anisotropy.

^{17}O Enrichment Studies. Figure 4 shows the Mo(V) EPR spectrum of native WT DMSO reductase exchanged into 47% (final) H_2^{17}O by diluting highly concentrated enzyme with enriched water, equilibrating for 3 h at 4 °C, and then adjusting E_h to ~ 60 mV. The Mo(V) EPR spectrum shows clear broadening of all features, with some partially resolved structure (Figure 4). Bray and Gutteridge³⁵ have reported a simple method for estimating the numbers of coupled ^{17}O nuclei with resolved or partly resolved hyperfine structure. In this method, EPR double integration and difference spectra are employed to estimate the fraction of Mo(V) which is unenriched; this is equal to $(1 - a)^n$ where a is the isotopic enrichment and n the number of coupled oxygens. Using this method, we find that a single ^{17}O is coupled to molybdenum in DMSO reductase. The most likely identity for this oxygen is a Mo–OH ligand, where the H is the exchangeable proton which is observed coupled to Mo(V) and the oxygen atom derives from protonation of the single Mo=O ligand of oxidized enzyme (see below). The computer simulation shown in Figure 4c, while not a perfect fit to the experimental data, clearly indicates anisotropic hyperfine coupling to a single ^{17}O (Table 1). There is only one report of a Mo(V) model complex with ^{17}O coupling from Mo–OH ligation.³⁶ This complex, in contrast to DMSO reductase, is a $[\text{Mo}=\text{O}]^{3+}$ species, and again caution should be used in comparing spin Hamiltonian parameters. Nevertheless, the Mo(V) EPR of the model compound³⁶ shows proton hyperfine and anisotropic ^{17}O hyperfine couplings of similar sizes, although slightly larger than those observed for DMSO reductase. Estimation of the anisotropic component of the DMSO reductase ^{17}O hyperfine coupling matrix³⁷ indicates an approximate oxygen p-orbital spin density of 0.05 electron, arguing for a

(35) Bray, R. C.; Gutteridge, S. *Biochemistry* **1982**, *21*, 5992–5999.

(36) Greenwood, R. J.; Wilson, G. L.; Pilbrow, J. R.; Wedd, A. G. *J. Am. Chem. Soc.* **1993**, *115*, 5385–5392.

(37) Goodman, B. A.; Raynor, J. B. *Adv. Inorg. Chem. Radiochem.* **1970**, *13*, 135–362.

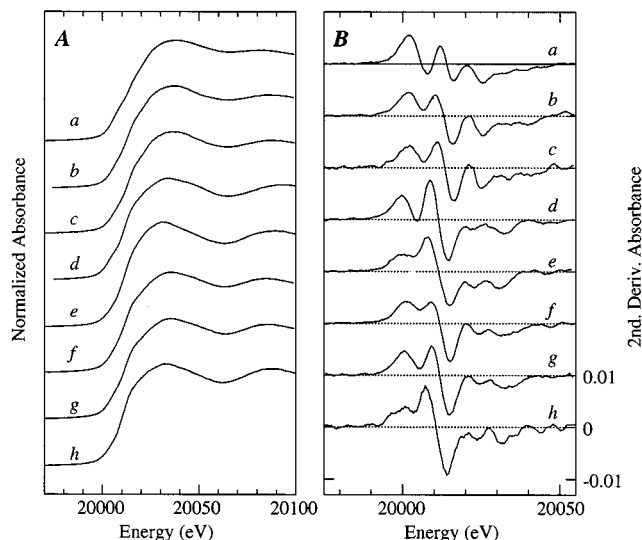


Figure 5. Molybdenum K-edge near-edge spectra (A) and corresponding second derivatives (B) of DMSO reductase. Traces a–e show spectra of native WT enzyme, while traces f–h show spectra of the S147C variant. Trace a shows the oxidized recombinant WT enzyme, trace b the oxidized native WT enzyme, trace c oxidized redox-conditioned (reduced then reoxidized) recombinant enzyme, trace d dithionite reduced native WT enzyme, trace e dimethyl sulfide reduced native WT enzyme, trace f as-isolated S147C enzyme, trace g redox-conditioned (reduced then reoxidized) S147C enzyme, and trace h dithionite-reduced S147C enzyme.

correspondingly small participation in the half-occupied ground-state molecular orbital.

Mo K-Edge Near-Edge X-ray Absorption Spectra. Figure 5 shows the Mo K-edge near-edge spectra of the different forms of DMSO reductase investigated. The spectra are broadly similar, with subtle differences that are highlighted by the second-derivative plot of Figure 5B. The pre-edge feature at about 20008 eV has been observed for other molybdenum enzymes.² This so-called oxo-edge feature is characteristic of a species possessing Mo=O groups (or to a lesser extent Mo=S); it arises from formally dipole-forbidden $1s \rightarrow 4d$ bound-state transitions to antibonding orbitals directed principally along Mo=O bonds.³⁸ While firm structural conclusions are not possible from analysis of these data, we note that the oxo-edge feature is most intense in the as-isolated recombinant WT DMSO reductase (Figure 5a), which argues for a higher number of these ligands in this sample.

Mo K-Edge EXAFS Spectra. Figure 6 shows the Mo K-edge EXAFS spectra, the best fits, and the corresponding Fourier transforms of recombinant WT, native WT, and the S147C variant DMSO reductases in oxidized and reduced reduced forms. The results of the curve-fitting analyses are summarized in Table 2. None of the very long (~ 3 Å) Mo–S EXAFS predicted from crystallographic studies⁹ were observed in any of the samples examined, although we note that these might be undetectable. We have previously reported¹³ that the oxidized native WT enzyme possesses a monooxo molybdenum site with approximately four Mo–S ligands.³⁹

In contrast to the case of the native WT enzyme,¹³ curve-fitting analysis of the EXAFS from the as-isolated recombinant WT enzyme indicates a novel dioxo species with two Mo=O at 1.72 Å and four Mo–S at 2.48 Å.⁴⁰ No improvement in the fit was obtained when additional light scatterers such as Mo–O

(38) Kutzler, F. W.; Natoli, C. R.; Misemer, D. K.; Doniach, S.; Hodgson, K. O. *J. Chem. Phys.* **1980**, *73*, 3274–3288.

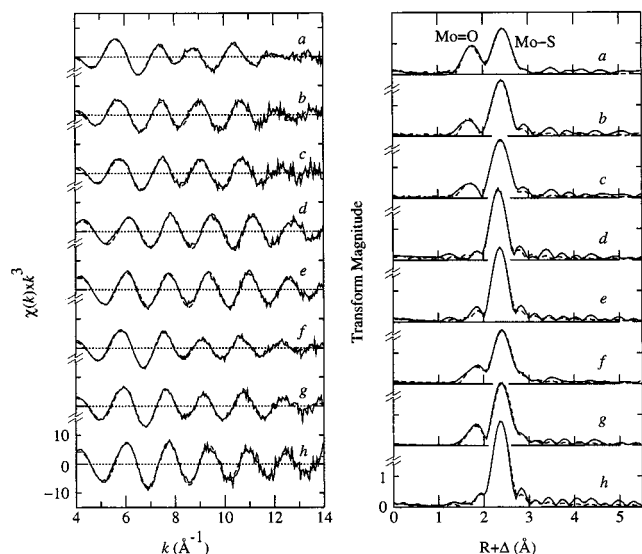


Figure 6. Mo K-edge EXAFS spectra and corresponding EXAFS Fourier transforms of DMSO reductase samples. In all cases, the solid lines show experimental data, while the broken lines show the best fits (Table 2). The EXAFS Fourier transforms have been phase-corrected for Mo–S backscattering. Traces a–e show spectra of native WT enzyme, while traces f–h show spectra of the S147C variant. Trace a shows the oxidized recombinant WT enzyme, trace b the oxidized native WT enzyme, trace c oxidized redox-conditioned (reduced then reoxidized) recombinant enzyme, trace d dithionite reduced native WT enzyme, trace e dimethyl sulfide reduced native WT enzyme, trace f as-isolated S147C enzyme, trace g redox-conditioned (reduced then reoxidized) S147C enzyme, and trace h dithionite reduced S147C enzyme.

were added to the refinements (Table 2). When the recombinant enzyme was reduced and then reoxidized (as with the Mo(V) EPR), the Mo K-edge EXAFS of the resulting protein was found to be indistinguishable from that of native WT enzyme (Figure 6, Table 2A). The original dioxo species could not be regenerated by air oxidation even after several hours. EXAFS studies of the tungsten-containing aldehyde oxidoreductase from *Pyrococcus furiosus*⁴¹ show that this enzyme can also exist as a dioxo or monooxo active site. Oxygen-inactivated enzyme possesses two W=O ligands,^{41,42} whereas the anaerobically purified and sulfide-activated forms of the enzyme contain one W=O.⁴² For the oxygen-stable DMSO reductase, the difference

(39) The Debye–Waller factor of 0.0033 Å² determined from curve-fitting is large for a Mo=O ligand, which (see discussion below) is expected to be about 0.0015 Å². We note that this is the least well determined parameter in the EXAFS curve-fitting analysis, as indicated by the 95% confidence limit of ± 0.0018 Å² (Table 2), which causes an overlap with the ideal value. In support of this, we find that curve-fitting analysis of five equivalent EXAFS data sets of the monooxo Mo thiolate complex [PPh₄][MoO(SPh)₄] (Bradbury, J. R.; Mackay, M. F.; Wedd, A. G. *Aust. J. Chem.* **1978**, *31*, 2423–2426) gave values for the Mo=O Debye–Waller factor ranging from 0.0017 to 0.0026 Å², with the lower values resulting from the data sets of highest quality.

(40) Confidence in the conclusion of a dioxo active site for the recombinant wild-type enzyme is reinforced by the fact that the decrease in fit error between one Mo=O and two Mo=O ligands is significantly improved when k^2 weighting is used to increase sensitivity to these ligands. This is because the EXAFS amplitude for an oxygen backscatterer is more pronounced at low k , while that for the Mo–S is more pronounced at high k . Thus, comparing refinements with one and two Mo=O, with k^3 weighting the fit improves by about 19% when two Mo=O ligands are assumed (from 0.309 to 0.259; Table 2) and by 44% when k^2 weighting is used (from 0.231 to 0.160). In either case, the intensity of the Mo=O peak in the EXAFS Fourier transform is only reproduced with two Mo=O ligands.

(41) George, G. N.; Prince, R. C.; Mukund, S.; Adams, M. W. W. *J. Am. Chem. Soc.* **1992**, *114*, 4, 3521–3523.

(42) George, G. N.; Prince, R. C.; Mukund, S.; Adams, M. W. W. Unpublished results.

between the recombinant WT dioxo protein and the native WT is likely due to the fact the former enzyme has never undergone redox-cycling (as part of catalytic turnover), whereas the latter enzyme certainly has, as the organism was grown on DMSO.

The lack of any observed trans-effects in the Mo–S bond lengths of the dioxo form of DMSO reductase clearly implies a nonoctahedral geometry. This is illustrated by Figure 7, which compares the Mo K-edge EXAFS Fourier transforms of the (approximately) octahedral complex MoO₂(diethyldithiocarbamate)₂⁴³ and that of dioxo recombinant WT DMSO reductase. The Fourier transform of the model compound spectrum clearly shows two distinct Mo–S peaks, corresponding to molybdenum thiolates that are cis and trans to the Mo=O groups with Mo–S bond lengths of 2.45 and 2.64 Å, respectively. As we have previously pointed out,¹³ similar arguments apply to the monooxo oxidized native WT protein, and a trigonal prismatic geometry^{9–12} of the type illustrated in Figure 8 seems most likely for both dioxo and monooxo forms of the enzyme.

Both the dithionite and DMS-reduced native WT DMSO reductase samples lack the ~ 1.7 Å Fourier transform peak indicative of Mo=O ligation, and curve-fitting indicates that both are desoxo species (Table 2A), with very similar molybdenum coordination environments. The DMS-reduced enzyme has approximately four Mo–S ligands at 2.36 Å and two Mo–O ligands at 1.94 and 2.14 Å. In both cases, attempts to include a molybdenum-oxygen ligand with a bond length appropriate for Mo=O refined to very high Debye–Waller factors, effectively removing this component from the fit.

The Mo K-edge EXAFS of the Ser147→Cys DMSO reductase variant is also shown in Figure 6f–h, and the curve-fitting results are summarized in Table 2B. The enzyme as isolated is a monooxo species with four Mo–S ligands (Table 2B). The fit was improved slightly by addition of a long Mo–O interaction at 2.2 Å. The Mo=O bond length of 1.71 Å is significantly longer than that of the native WT enzyme at 1.68 Å, and the Mo–S bond length is slightly shorter (2.42 Å vs 2.44 Å). This gives a bond valence sum $V^{13,44,45}$ of 5.9, which is consistent with the supposed oxidation state of Mo(VI). The Mo=O Debye–Waller factor of 0.0041 Å² is large, suggesting some active site heterogeneity. The Mo–S Debye–Waller factor of 0.0062 Å² is also consistent with some disorder in Mo–S bond lengths. Inclusion of an additional oxygen at 2.23 Å required a very large Debye–Waller factor (0.031 Å²), effectively removing this contribution from the fit. After the S147C protein had been reduced with 5 mM dithionite plus 0.1 mM methyl viologen and subsequently reoxidized, the Mo=O bond length was decreased to 1.70 Å, with a slightly shorter Mo–S bond length of 2.40 Å. The Mo–S coordination was apparently increased from 4 to 5, and an additional oxygen (at 2.00 Å) improved the fit slightly.⁴⁶ The active site of the S147C variant thus exhibits redox-conditioning similar to that observed with the recombinant WT protein. EXAFS curve-fitting analysis of the dithionite-reduced enzyme indicated a desoxo active site with approximately five Mo–S ligands and one Mo–O (Table 2B). Added DMS did not reduce the S147C enzyme, as judged by the electronic spectrum. Enzyme reduced by dithionite and methyl viologen in the presence of DMS gave EXAFS data that

(43) (a) Kopwille, A. *Acta Chem. Scand.* **1972**, *26*, 2941. (b) Berg, J. M.; Hodgson, K. O. *Inorg. Chem.* **1980**, *19*, 2180–2181.

(44) (a) Brown, I. D.; Altermat, D. *Acta Crystallogr.* **1985**, *B41*, 244–247. (b) Brese, N. E.; O’Keeffe, M. *Acta Crystallogr.* **1991**, *B47*, 192–197.

(45) Thorp, H. H. *Inorg. Chem.* **1992**, *31*, 1583–1588.

(46) We note that discrimination of four Mo–S ligands from five Mo–S ligands is bordering on the limits of accuracy of the technique, and our coordination numbers discussed above are thus somewhat tentative.

Table 2. EXAFS Curve-Fitting Results^a

sample	Mo=O			Mo-S			Mo-O ^b			error ^c
	<i>N</i>	<i>R</i>	σ^2	<i>N</i>	<i>R</i>	σ^2	<i>N</i>	<i>R</i>	σ^2	
(A) Native and Recombinant Wild-Type DMSO Reductase										
wild-type Mo(VI)	1	1.683(6)	0.0033(6)	4	2.435(1)	0.0041(1)	1	1.920(15)	0.0067(17)	0.323^d
recombinant Mo(VI) as isolated	1	1.724(3)	0.0016(3)	4	2.475(2)	0.0055(2)				0.309
	2	1.722(3)	0.0044(3)	3	2.475(2)	0.0040(2)				0.292
	2	1.722(3)	0.0045(3)	4	2.475(2)	0.0055(2)				0.259
	2	1.722(3)	0.0044(3)	5	2.475(2)	0.0070(2)				0.263
	2	1.722(3)	0.0045(3)	4	2.476(2)	0.0055(2)	1	2.156(66)	0.0276(149)	0.259
wild-type Mo(IV)				3	2.333(2)	0.0022(2)	1	2.160(17)	0.0037(15)	0.221^d
wild-type DMS-reduced Mo(IV)							1	1.921(8)	0.0040(9)	
				4	2.361(1)	0.0030(1)				0.290
				4	2.361(1)	0.0031(1)	1	1.943(5)	0.0020(5)	0.245
				4	2.361(1)	0.0029(1)	2	1.964(9)	0.0091(12)	0.271
				3	2.361(1)	0.0018(1)	1	1.938(6)	0.0024(6)	0.300
				4	2.362(1)	0.0032(1)	1	1.944(5)	0.0020(5)	0.230
							1	2.144(16)	0.0063(2)	
(B) S147C DMSO Reductase										
S147C Mo(VI) as isolated	1	1.713(5)	0.0043(5)	5	2.419(1)	0.0062(1)				0.238
	1	1.712(5)	0.0042(5)	4	2.418(1)	0.0049(1)				0.255
	1	1.712(5)	0.0042(5)	4	2.421(2)	0.0050(2)	1	2.194(22)	0.0096(28)	0.232
	1	1.714(5)	0.0043(5)	5	2.419(1)	0.0063(1)	1	2.227(88)	0.0306(175)	0.237
S147C Mo(VI) redox-cycled	1	1.698(4)	0.0027(4)	4	2.400(1)	0.0038(1)				0.266
	1	1.698(4)	0.0028(4)	5	2.400(1)	0.0051(1)				0.261
	1	1.699(4)	0.0028(4)	4	2.401(1)	0.0039(1)	1	2.100(38)	0.0108(68)	0.259
	1	1.703(4)	0.0029(4)	5	2.401(1)	0.0050(1)	1	2.000(12)	0.0070(15)	0.251
S147C Mo(IV)				4	2.368(2)	0.0024(2)				0.344
				5	2.368(2)	0.0035(2)				0.321
				6	2.368(2)	0.0045(2)				0.325
				5	2.371(2)	0.0035(2)	1	2.119(20)	0.0059(3)	0.314

^a Coordination number *N*, interatomic distance *R* (Å), and (thermal and static) mean-square deviation in *R* (the Debye–Waller factor) σ^2 (Å²). The values in parentheses are the estimated standard deviations (precisions) obtained from the diagonal elements of the covariance matrix. We note that the accuracies will always be somewhat larger than the precisions, typically ± 0.02 Å for *R* and $\pm 20\%$ for *N* and σ^2 . Fits shown in boldface type represent the best fits obtained for the samples. ^b Note that EXAFS cannot readily distinguish between scatterers of similar atomic numbers, such as chlorine and sulfur or nitrogen and oxygen. ^c The fit error is defined as $\sum k^6(\chi_{\text{exptl}} - \chi_{\text{calcd}})^2 / \sum k^6 \chi_{\text{exptl}}^2$. ^d Data taken from ref 13.

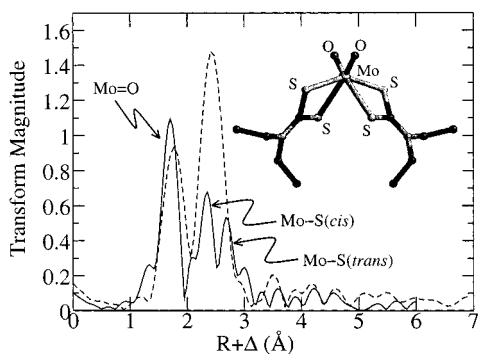


Figure 7. Comparison of the Mo K-edge EXAFS Fourier transforms of MoO₂(diethyldithiocarbamate)₂ (solid line) and dioxo recombinant WT DMSO reductase (broken line). In both, the metal is coordinated by two Mo=O and four Mo-S ligands. In the (approximately) octahedral model compound, trans effects from the Mo=O groups cause elongation of some Mo-S bonds, and the lack of this in the enzyme data indicates a nonoctahedral coordination geometry.

were not significantly different from those of enzyme reduced with dithionite and methyl viologen alone.

Discussion

The EXAFS curve-fitting results presented herein and previously¹³ show the presence of approximately four Mo-S ligands for native WT DMSO reductase. This is consistent with the presence of two pterin dithiolene ligands.²³ The data also unambiguously indicate that the Mo(VI) enzyme contains a monooxo molybdenum site and that this oxo group is converted to a Mo-O ligand upon reduction with either dithionite or DMS,

as shown diagrammatically in Figure 8. In agreement with this, EPR suggests the presence of a single Mo-OH ligand in the Mo(V) oxidation state. The resonance Raman studies recently reported by Garton et al.¹⁶ support these conclusions.¹³

There are important differences between the DMS- and dithionite-reduced active sites. When DMS is used as a reductant, DMSO becomes coordinated to molybdenum, and there are clearly four Mo-S ligands. When dithionite is used as the reductant, the EXAFS suggests three rather than four thiolate ligands, which is in excellent agreement with the structure for dithionite-reduced enzyme proposed by McAlpine et al.¹¹ We note, however, that since EXAFS-derived coordination numbers typically have an uncertainty of $\pm 20\%$, it is difficult to distinguish between three and four Mo-S ligands. Nevertheless, the bond length trends (Table 2) support three Mo-S ligands for dithionite-reduced enzyme.¹³ On the other hand, the resonance Raman data of Garton et al.¹⁶ argue for four Mo-S from two slightly different dithiolene ligands for all forms of the enzyme studied. This area clearly needs further study.

Perhaps unexpectedly, the recombinant WT enzyme as isolated exhibits a novel dioxo coordination (Figure 8), with apparently no coordinating amino acid side chain residue. Redox cycling converts the enzyme to a monooxo structure indistinguishable from the enzyme isolated from *R. sphaeroides*. The difference is probably due to the fact that the recombinant enzyme has never undergone catalytic turnover, a finding that has important implications for understanding the insertion of the cofactor and assembly of a functional active site.

The EPR and EXAFS data of the Ser147→Cys variant enzyme are consistent with Cys147 as a ligand on molybdenum

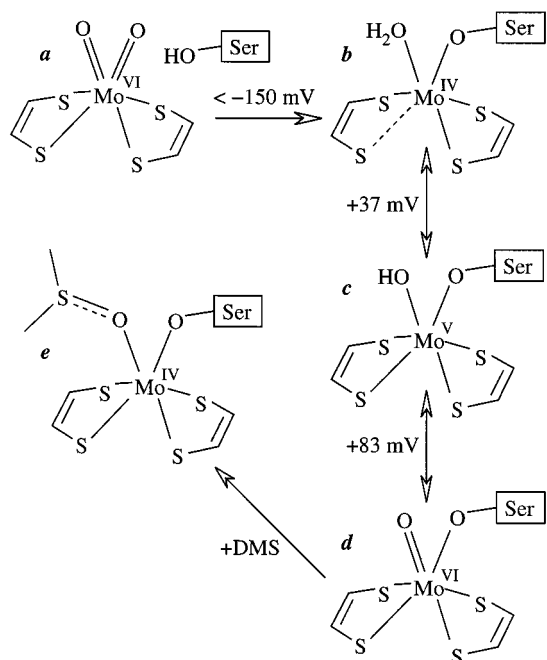


Figure 8. Proposed structures of, and relationships among, the Mo(VI), Mo(V), and Mo(IV) species of native WT DMSO reductase. Midpoint potentials (pH 8.5) as determined by redox titrations (Figure 3) are given where appropriate. **a** shows the postulated structure of the recombinant WT as-isolated Mo(VI) enzyme, **b** that of the fully reduced Mo(IV) enzyme, **c** the Mo(V) EPR signal-giving species, **d** the oxidized Mo(VI) form for both redox-conditioned recombinant WT and native WT enzymes, and **e** the postulated structure of DMS-reduced enzyme. For structures **b** and **c** the shorter of the two Mo–O bond lengths (Table 2) is likely to be the Mo–O–Serine. For structure **e**, a search of the Cambridge Structure Data Base suggests that the longer of the two Mo–O is likely to be the Mo–O–DMS ligand.

in all oxidation states other than that of the as-isolated enzyme (Figure 9). This in turn supports the crystallographic identification of serine as a ligand of molybdenum in native WT enzyme (Figure 8). Similar to the recombinant WT enzyme, the S147C variant shows structural changes on redox cycling, which probably involves the formation of the Mo–S(Cys147) bond. Unlike the native WT enzyme, the as-isolated variant has a monooxo Mo(VI) active site and probably a long Mo–O ligand, shown as a coordinated water in Figure 9.

Our results have some implications for related molybdenum enzymes. As has been previously discussed (e.g., ref 2), Ser147 is part of a peptide sequence that is conserved among prokaryotic molybdenum enzymes. The Ser147 residue of DMSO reductase is replaced by cysteine in formate dehydrogenases from *Wolinella succinigenes* and *Methanobacterium formicicum* and in nitrate reductases from a variety of sources (including *E. coli*) by selenocysteine in *E. coli* formate dehydrogenase² and remains a serine in *R. sphaeroides* biotin sulfoxide reductase and in *E. coli* DMSO reductase.² These amino acids are likely to be ligands on molybdenum in their respective enzymes. Thus we might have expected that the properties of S147C DMSO reductase would resemble those of *E. coli* nitrate reductase, which is the best studied of the cysteine-containing enzymes. Not surprisingly, S147C DMSO reductase does not possess any nitrate reductase activity (although it has gained adenine *N*-oxide reductase activity!), but the Mo(V) EPR properties are also distinctly different.^{47–49} Instead (as previously pointed out by Bennet et al.²⁰), the EPR of native WT DMSO reductase is very

(47) George, G. N.; Bray, R. C.; Morpeth, F. F.; Boxer, D. H. *Biochem. J.* **1985**, *227*, 925–931.

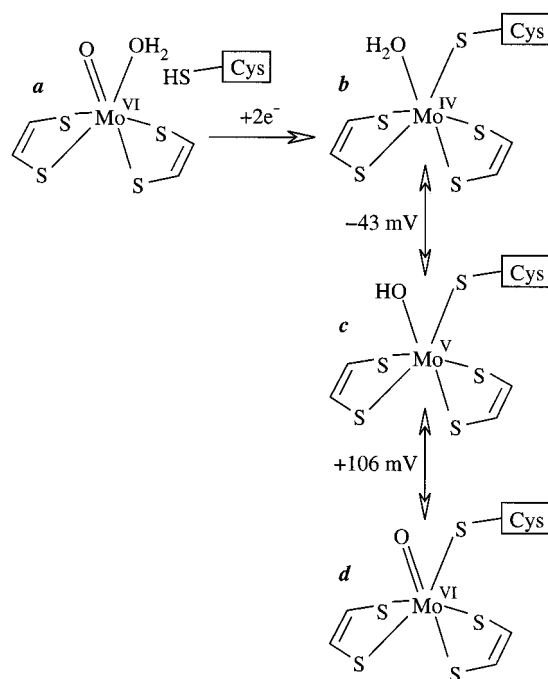


Figure 9. Proposed structures of, and relationships among, the Mo(VI), Mo(V), and Mo(IV) species of Ser147→Cys DMSO reductase. Midpoint potentials are those determined by redox-titrations (Figure 3). **a** shows the postulated structure for the oxidized Mo(VI) variant as isolated, **b** the fully reduced Mo(IV) enzyme, **c** the major Mo(V) EPR signal-giving species, and **d** the oxidized Mo(VI) form of the variant after redox cycling.

similar to that of the *E. coli* nitrate reductase anion-bound low-pH species.⁴⁷ It is of course possible that the cysteine is not a ligand in *E. coli* nitrate reductase, but if it is, then the coordinating amino acid cannot be the sole determinant of active-site properties and structure.⁵⁰

A recent EXAFS study of *R. capsulatus* DMSO reductase by Baugh et al.¹⁴ is in substantial disagreement with our findings (Table 2A). These workers studied the enzyme in oxidized, dithionite-reduced, and DMS-reduced forms.¹⁴ Their interpretations are at odds both with our previous analysis^{13,51} and with the analysis presented herein but are in substantial agreement with the crystal structure studies of Bailey and co-workers.^{11,12} Their EXAFS analysis includes eight, five, and nine components, respectively, for the oxidized, dithionite-reduced, and DMS-reduced forms, with contributions from directly coordi-

(48) George, G. N.; Turner, N. A.; Bray, R. C.; Morpeth, F. F.; Boxer, D. H.; Cramer, S. P. *Biochem. J.* **1989**, *259*, 693–700.

(49) Cramer, S. P.; Solomonson, L. P.; Adams, M. W. W.; Mortenson, L. E. *J. Am. Chem. Soc.* **1984**, *106*, 1467–1471.

(50) We note that no resolved ¹⁷O hyperfine coupling was detected in the *E. coli* nitrate reductase Mo(V) nitrate complex EPR signal in experiments using isotopically enriched nitrate,⁴⁷ which suggests that nitrate is not a ligand of Mo. On the other hand, the fluoride complex shows well-resolved ¹⁹F hyperfine structure, suggesting anion ligation. The similarity of the DMSO reductase Mo(V) EPR, which lacks sensitivity to anions, suggests that anions are probably not ligated directly to Mo in *E. coli* nitrate reductase and that the observed ¹⁹F hyperfine structure could arise primarily from dipole–dipole splittings from fluoride bound in an anion binding pocket.

(51) The EXAFS analysis of Baugh et al.¹⁴ used the statistical significance test developed by Joyner et al.⁵² (a modified *F* test⁵³). Unfortunately the *F* test is inappropriate for comparison of two models which have been independently refined, as is the case with EXAFS curve-fitting.^{52,54}

(52) Joyner, R. W.; Martin, K. J.; Meehan, P. *J. Phys. C. Solid State Phys.* **1987**, *20*, 4005–4012.

(53) Sachs, L. *Applied Statistics*, 2nd ed.; Springer-Verlag: New York, Berlin, Heidelberg, Tokyo, 1984.

(54) George, G. N. *J. Biol. Inorg. Chem.* **1997**, *2*, 790–796.

nated Mo–S and Mo–O ligands, long-distance Mo···C interactions from the Ser147 and the pterin dithiolene ligands, and, in the case of DMS-reduced enzyme, an additional remote sulfur from bound DMS.^{14,55} These analyses have unusually large numbers of variables for EXAFS, and inspection of their analysis reveals that most components have been refined with physically unreasonable Debye–Waller factors. Thus, five of the eight interactions included for the oxidized enzyme have Debye–Waller factors outside a physically reasonable range⁵⁶ and two are so large as to essentially eliminate their EXAFS. For the parameters reported,^{14,55} the EXAFS from one of the three Mo–O and from one Mo–S are almost in phase throughout the k range of the data, while that from the short Mo–O is essentially out of phase with that from the third Mo–O. These factors, combined with the use of physically unreasonable Debye–Waller factors, suggest an incorrect assignment of backscatterers.⁵⁴

(55) We cannot reproduce the calculated EXAFS spectra reported by Garner and co-workers¹⁴ for oxidized and dithionite-reduced DMSO reductase, and it is likely that there are typographical errors in the parameters reported. Only for the DMS-reduced enzyme can we accurately reproduce the form of their EXAFS simulations. We also note that a fully quantitative approach is not possible as the data reported by these workers have no ordinate scale.

(56) The Debye–Waller factor σ^2 is defined as the mean-square deviation of the average bond length R . Larger values for σ^2 cause the EXAFS to be damped at higher k , relative to EXAFS with small σ^2 . Thus, the effects of the Debye–Waller factor are similar to those of the thermal parameter in X-ray crystallography, and high values will obscure a particular atom. Phenomenologically, σ^2 can be represented as a sum of vibrational and static components $\sigma^2 = \sigma_{\text{vib}}^2 + \sigma_{\text{stat}}^2$. The contribution σ_{stat}^2 arises from structural disorder in bond lengths differing by less than the EXAFS resolution (which is given approximately by $\pi/2k$), and for a single absorber–backscatterer pair, σ_{stat}^2 will be zero. In the case of a diatomic harmonic oscillator σ_{vib}^2 is simply given by

$$\sigma_{\text{vib}}^2 = \left(\frac{h}{8\pi^2\mu\nu} \right) \coth\left(\frac{h\nu}{2kT} \right)$$

where ν is the vibrational frequency of the bond–stretch vibration, μ is the reduced mass, k is Boltzmann's constant, and T is temperature. This approximation should work moderately well for molybdenum EXAFS as the absorber atom is much more massive than the backscatterer. Using ν for known compounds, this leads to estimated lower limits for Debye–Waller factors of about 0.0015 and 0.0020 Å² for Mo=O and Mo–S, respectively. As has been previously pointed out by Cramer et al.,⁵⁷ in the case of T_d (and O_h) symmetry, it is trivial to calculate σ_{vib}^2 exactly using vibrational spectra. Thus, for the tetrahedral anion MoO_4^{2-} σ_{vib}^2 is 0.00150 Å².⁵⁸ Debye–Waller factors are known to increase with increasing bond length R ,⁵⁷ and the harmonic oscillator approximation can be used to estimate this using Badger's rule to estimate the bond length dependency of ν . Thus, for Mo–O with $R = 1.90$ Å we calculate σ_{vib}^2 of 0.0022 Å² and with $R = 2.0$ Å, σ_{vib}^2 of 0.0025 Å². We note that only slight changes in σ_{vib}^2 are expected for Mo=O and Mo–S between 10 and 77K. An upper limit for σ_{stat}^2 can be estimated from the coordination number and the EXAFS resolution. For N atoms at an average distance R and individually at R_i

$$\sigma_{\text{stat}}^2 \approx \frac{1}{N} \sum (R_i - R)^2$$

where $|R_i - R|$ is less than or equal to the EXAFS resolution of approximately $\pi/2k$. For two dissimilar (unresolved) Mo–S bonds and an EXAFS k range of 12 Å⁻¹, a maximum σ_{stat}^2 is 0.0043 Å², combining with σ_{vib}^2 to give an overall upper limit for σ^2 of 0.0063 Å². It is important to note that, among the parameters available from quantitative EXAFS analysis, σ^2 is not well determined. Thus, being somewhat generous with our limits, σ^2 values of less than 0.0015 Å² for Mo=O bonds are chemically unreasonable, as are values greater than 0.0050 Å². Indeed, the damping of the EXAFS with a Debye–Waller factor of 0.01 Å² (or larger) is generally sufficient to effectively eliminate this EXAFS contribution from the total.

(57) Cramer, S. P.; Wahl, R.; Rajagopalan, K. V. *J. Am. Chem. Soc.* **1981**, *103*, 7721–7727.

(58) (a) Muller, A.; Nagarajan, G. Z. *Naturforsch., B.: Anorg. Chem., Org. Chem., Biochem., Biophys.* **1966**, *21B*, 508–512. (b) Nagarajan, G. *Acta Phys. Pol.* **1965**, *6*, 875–882.

Garner and co-workers' analysis of the dithionite-reduced enzyme¹⁴ is in partial agreement with ours,¹³ with four Mo–S and two different Mo–O. However, one of their Mo–O is refined with a very long bond length of 2.5 Å, contributing only 5% of the total amplitude, while the other has an unreasonably large Debye–Waller factor and contributes less than 4% of the total. Thus, their EXAFS analysis of the dithionite-reduced sample is dominated by Mo–S at about 2.36 Å, which is only a little longer than our estimate of 2.33 Å (Table 2A).¹³

In contrast with our findings (Table 2A), Baugh et al.¹⁴ conclude that DMS-reduced enzyme possesses one Mo=O ligand with a bond length of 1.69 Å. However, this is again refined with the physically unreasonable Debye–Waller factor of 0.014 Å², suggesting a root-mean-square displacement 2 orders of magnitude greater than that expected.⁵⁶ This Mo=O thus contributes a little less than 2% of the total EXAFS amplitude in their analysis. In fact, of the nine components refined in their analysis, only two individually contribute more than 6% of the total amplitude, and all but these two can therefore be reasonably neglected. These interactions (one Mo–O at 1.91 Å and two Mo–S at 2.37 Å) have refined Debye–Waller factors that are unreasonably small (both 0.001 Å²), the latter undoubtedly as a consequence of the coordination number being too low.

Thus, when allowance is made for the analysis methods used by Garner and co-workers,¹⁴ it is clear that our analysis (Table 2A) and theirs, in fact, point to the same conclusions. Neither indicates the dioxo oxidized or monooxo DMS-reduced active site suggested from crystallography by Bailey and co-workers.¹²

Finally we will address the different proposed crystallographic structures of the active site of DMSO reductase^{9–12} in light of the EXAFS spectroscopy, and bearing in mind chemically reasonable geometry.

It is of course possible that the different DMSO reductase crystal structures^{9–12} reflect genuine structural differences between the different preparations of the proteins. However, at least for solution samples, the weight of spectroscopic evidence argues against this, at least for the structures of Schindelin et al.⁹ and Bailey and co-workers.^{11,12} The similarity of the Mo(V) EPR, the optical spectra, the MCD spectra, and now the EXAFS data all seem to suggest similar active-site structures. In our discussion, we will use the nomenclature of Schindelin et al.⁹ for the sulfur and pterin atoms.

Although the structures of oxidized and reduced enzymes described by Schindelin et al.⁹ are in partial qualitative agreement with the EXAFS data, they are chemically unusual. The oxidized enzyme is five-coordinate with three Mo–S ligands, one Mo=O, and one oxygen donor from Ser147 (Figure 10a). The two sulfur ligands from the P pterin have bond lengths of 2.51 and 2.49 Å (S1 and S2, respectively), and the bond to S2 of the Q pterin has a bond length of 2.51 Å. The single Mo=O is rather close to S2 of the P pterin at 2.25 Å. As has been previously pointed out,⁵⁴ molybdenum is ligated in less than half of its coordination sphere with four of the five ligands approximately on the plane normal to the Mo–S1(P pterin) bond. The reduced site described by Schindelin et al.⁹ is also rather unusual (Figure 10b). Here the Mo is effectively three-coordinate with only the P pterin dithiolene and the Ser147 O_γ being less than 3 Å from Mo. There are no other reports of three-coordinate high-valent molybdenum complexes with sulfur donors in the literature.

The structure determined by Schneider et al.¹⁰ of *R. capsulatus* DMSO reductase is shown in Figure 10c. These workers conclude that the oxidized molybdenum site in their preparations

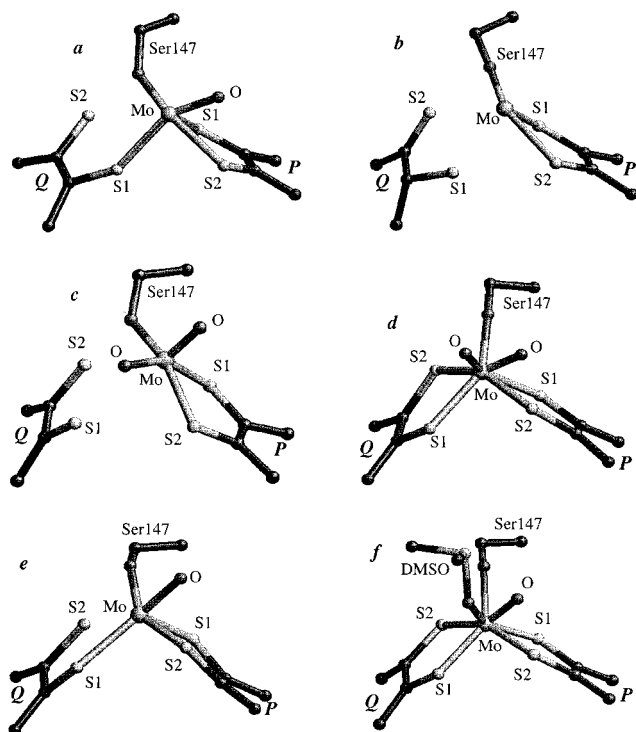


Figure 10. Active-site structures proposed from X-ray crystallographic studies of DMSO reductase from *R. sphaeroides* and *R. capsulatus*. Coordinates were taken from the Brookhaven Protein Data Bank using entries 1CX5, 1CXT, 1DMS, 1DMR, 2DMR, and 4DMR for structures a–f, respectively. Plots a and b show the *R. sphaeroides* structures for oxidized (a) and dithionite-reduced (b) enzyme of Schindelin et al.⁹ Plot c shows the oxidized *R. capsulatus* structure of Schneider et al.¹⁰ Plots d–f show the structures of Bailey and co-workers^{11,12} for the *R. capsulatus* enzyme in oxidized (d),¹¹ dithionite-reduced (e),¹¹ and DMS-reduced (f) forms.¹²

of *R. capsulatus* DMSO reductase is very similar to that of desulfo xanthine oxidases and aldehyde oxidases.⁸ Of the two cofactor dithiolenes, only the P pterin is coordinated to molybdenum and the active-site coordination is completed by an oxygen ligand from serine 147 and two terminal oxygens. While being chemically the least unconventional of the crystallographically proposed sites, its structure still contains unusual features. In particular, the O=Mo=O angle is rather small at 94° and the two Mo–S bond lengths are quite different at 2.5 and 2.3 Å, for Mo–S1 and Mo–S2, respectively. Such a difference would be easily resolved in Mo K-edge EXAFS. As previously discussed,^{10,54} the structural conclusions of Schneider et al.¹⁰ are in part⁵⁹ consistent with the Mo(V) EPR spectroscopy of Bray and co-workers,²⁰ which indicated that DMSO reductase can exist in a form similar to desulfo xanthine oxidase, although this is probably not a native form.²⁰ We note in passing that the Mo–S(Q pterin) distances of Schneider et al.¹⁰ differ by only tenths of an angstrom from those given for the reduced *R. sphaeroides* protein by Schindelin et al.⁹ (Mo–S1Q 3.5 Å vs 3.0 Å and Mo–S2Q 3.9 Å vs 3.8 Å), and yet the two groups deduce quite different formal chemistries for this group in the active site.

(59) As previously discussed^{10,13,20,54} the similarity of the *D. desulfuricans* low-*g* type 1 signal to the slow signal of desulfo xanthine oxidase²⁰ argues for a (molybdopterin)₂Mo=O(OH)₂ coordination for both signal-giving species.^{10,13,54} Given the exquisite sensitivity of Mo(V) spin Hamiltonian parameters to structure, it seems unlikely that a (molybdopterin)₂Mo=O(OH)(O–Ser) coordination would give similar EPR parameters. Possibly, the low-*g* type 2 signal²⁰ corresponds to the reduced form of the structure described by Schneider et al.¹⁰

The crystal structure analyses of Bailey and co-workers for *R. capsulatus* DMSO reductase^{11,12} are illustrated in Figure 10d–f. The seven-coordinate geometry of the oxidized (Figure 10d) and DMS-reduced (Figure 10f) enzymes is unusual for molybdenum, although not without precedent (e.g., see ref 60). A closer examination of the crystal structure indicates more unusual features, all centered around one of the Mo=O ligands. In the structure of the oxidized enzyme (Figure 10d), the two oxo groups are separated by only 1.94 Å and one is only 1.90 Å from one of the pterin dithiolene sulfurs (S2 of the P pterin) with a S–Mo=O angle of 49°. Both of these distances are much less than the sum of the van der Waals radii of the atoms concerned. The O=Mo=O angle of 70° is also very small; of the large number of dioxomolybdenum species known, the average O=Mo=O angle is 106°,⁶¹ and there are no reported complexes for which this angle is less than 95°. The structure proposed for the dithionite-reduced enzyme¹¹ is, on the other hand, chemically reasonable (Figure 10e). Unfortunately, this is not the case with the DMS-reduced enzyme (Figure 10f). Here the Mo=O ligand is separated from the P pterin S1 sulfur by 2.09 Å, from O_γ of Ser147 by 1.99 Å, and from the oxygen of bound DMSO by 1.90 Å. Again, these distances are less than the sum of van der Waals radii. The Mo=O is unreasonably crowded and cannot be coordinated in the location proposed.

Recently, additional high-resolution (1.35 Å) crystallographic data on *R. sphaeroides* DMSO reductase have become available.^{63,64} From this work come the interesting suggestions of a cofactor sulfenic acid (R–S–OH) coordinated to molybdenum and of one distant cysteine (Cys219) oxidized to the sulfinic acid (R–SOOH). While sulfenic acid coordination is certainly a chemically novel suggestion,⁶⁵ implying some interesting possible catalytic mechanisms, there are reports of chemically related models.⁶⁶ Future X-ray spectroscopy at the sulfur K edge⁶⁷ will address these interesting possibilities, and preliminary results support the suggestion of a cysteine sulfinic acid residue in some forms of the enzyme.

Not surprisingly, the different proposed active-site structures have led to quite different suggested mechanisms for the enzyme. Isotopic labeling⁶⁸ and resonance Raman spectroscopy¹⁶

(60) Dirand, J.; Ricard, L.; Weiss, R. *Transition Met. Chem.* **1975**, *1*, 2–5.

(61) Stiefel, E. I. In *Comprehensive Coordination Chemistry*; Wilkinson, G., Ed.; Pergamon Press: Oxford, U.K., 1987; pp 1375–1420.

(62) The O=Mo=O angle in MoO₂(tetra-*p*-tolylporphyrinate) is 95.1° (Menzen, B. F.; Bonnet, M. C.; Ledon, H. J. *Inorg. Chem.* **1980**, *19*, 2061–2066). In this case strong steric constraints force a smaller than normal bond angle and the large deviations of the porphyrin ring from planarity illustrate the contortions that can be tolerated to maintain the cis dioxo geometry.

(63) Rees, D. C.; Hu, Y.; Kisker, C.; Schindelin, H. *J. Chem. Soc., Dalton Trans.* **1997**, 3909–3914.

(64) Schindelin H. Personal communication.

(65) Sulfenic acids (R–S–OH) are chemically unstable and are not known as free acids, but are known mostly from their derivatives, e.g. sulfonyl halides (R–S–Cl). Nevertheless, biological sulfenic acids are known, and in particular a cysteine sulfenic acid is the redox center in streptococcal NADH peroxidase (Stehle, T.; Ahmed, S. A.; Claiborne, A.; Schultz, G. E. *J. Mol. Biol.* **1991**, *221*, 1325–1344). The possibility of derivitization of a cofactor dithiolene might provide an expansion for the observations of Bastian et al. (Bastian, N. R.; Foster, M. J. P.; Pope, J. C. *Biofactors* **1995**, *5*, 5–10) of modified Mo(V) EPR and optical spectra in the presence of NO and related compounds.

(66) Sulfines (RR'C=S=O) are well-known as transition metal ion ligands. A binuclear molybdenum complex with μ_2 -phenylsulfinyl ligands has been reported (Vasyutinskaya, E. A.; Eremenko, I. L.; Pasyanski, A. A.; Yanovskii, A. I.; Struchkov, Yu. T. *Zh. Neorg. Khim.* **1991**, *36*, 1707–1709).

(67) Pickering, I. J.; Prince, R. C.; Divers, T.; George, G. N. *FEBS Lett.* accepted for publication.

(68) Schultz, B. E.; Hille, R.; Holm, R. H. *J. Am. Chem. Soc.* **1995**, *117*, 827–828.

have demonstrated that DMSO reductase uses an oxygen transfer mechanism where the oxygen of DMSO is transferred to molybdenum as a Mo=O group in the oxidized enzyme. Schindelin et al.⁹ suggest that changes in Mo-S ligation are important in driving the catalytic cycle. In contrast, Garton et al.¹⁶ have proposed a mechanism in which the Mo-S coordination is invariant throughout the catalytic cycle. Finally, Garner, Bailey, and co-workers^{11,12,14} have proposed a mechanism in which Mo-S ligation is invariant and a spectator oxo group⁶⁹ assists in oxygen atom transfer. Since the active site clearly lacks the additional oxo group, this mechanism can be discounted. Overall, the mechanism proposed by Garton et al.¹⁶ is the most consistent with our data, although some changes in Mo-S ligation are suggested during catalysis by the EXAFS data.¹³

In conclusion, the crystal structures of Schindelin et al.⁹ and McAlpine et al.^{11,12} are not in quantitative agreement with the available spectroscopic data and in some cases are chemically impossible. And while the structure of Schneider et al.¹⁰ is consistent with the Mo(V) EPR spectroscopy of Bray and co-

(69) Rappe, A. K.; Goddard, W. A. *J. Am. Chem. Soc.* **1982**, *104*, 3287-3294.

(70) We note that there is a clear difference between chemically unusual or novel and chemically unreasonable; the active sites of very many metalloproteins can be considered to be chemically unusual.

workers, it still possesses some chemically unusual features.⁷⁰ Thus, while protein crystallography is invaluable in revealing the overall protein structure and the general environment of the metal site, a detailed understanding of the active site and its catalysis will require an integration of information from a broad range of spectroscopies.

Acknowledgment. The Stanford Synchrotron Radiation Laboratory was funded by the Department of Energy, Office of Basic Energy Sciences. The Biotechnology Program was supported by the National Institutes of Health, Biomedical Research Technology Program, Division of Research Resources. Further support was provided by the Department of Energy, Office of Biological and Environmental Research. Research at Duke University was supported by the National Institutes of Health, Grant GM00091 (K. V. R.). We are indebted to Martin J. George of SSRL for use of his data collection software and to Ingrid J. Pickering of SSRL for assistance with data collection. We thank Professor Robert Huber for allowing us access to the coordinates of *R. capsulatus* DMSO reductase in advance of deposition in the Brookhaven Data Base and Professor Charles Young for the gift of a sample of MoO₂(diethyl-dithiocarbamate)₂.

JA982843K